

**Asymmetric grain distribution in phthalocyanine thin films**

K. Paul Gentry and Thomas Gredig\*

*Department of Physics and Astronomy, California State University–Long Beach, 1250 Bellflower Boulevard, Long Beach, California 90840, USA*

Ivan K. Schuller

*Department of Physics and Astronomy, University of California–San Diego, 9500 Gilman Drive, La Jolla, California 92093, USA*

(Received 8 July 2009; revised manuscript received 24 October 2009; published 30 November 2009)

Many electronic and optical properties of organic thin films depend on the precise morphology of grains. Iron phthalocyanine thin films are grown on sapphire substrates at different temperatures to study the effect of grain growth kinematics and to experimentally quantify the grain size distribution in organic thin films. The grain size is measured with an atomic force microscope and the data is processed and analyzed with well-known image segmentation algorithms. For relevant statistics, over 3000 grains are evaluated for each sample. The data show pronounced asymmetric grain growth with increasing deposition temperature from almost spherical grains at room temperature to elongated needlelike shapes at 260 °C. The average size along the major axis increases from 35 to 200 nm and along the minor axis from 25 to 90 nm. The distribution is almost symmetric at low-deposition temperatures, but becomes lognormal at higher temperatures. Strikingly, the major axis and minor axis of the elliptically shaped grains have different distributions at all temperatures due to the planar asymmetry of the molecule.

DOI: [10.1103/PhysRevB.80.174118](https://doi.org/10.1103/PhysRevB.80.174118)

PACS number(s): 61.66.Hq, 81.15.Hi, 68.55.ag, 68.37.Ps

**I. INTRODUCTION**

Recently, there has been a growing interest in polycrystalline organic semiconductor thin films due to many intriguing new applications that include chemical sensors, organic transistors, and flexible photovoltaic devices.<sup>1–3</sup> Clearly for these applications, the nucleation and grain growth mechanism play an important role in predetermining the final electronic, optical, and even magnetic characteristics of an organic thin film.<sup>4–7</sup> The characteristic length scale of crystallites can vary in size from a few nm to a few  $\mu\text{m}$  and are measured by scanning electron microscopy, transmission electron microscopy, x-ray diffraction, and atomic force microscopy (AFM). Furthermore, the grain orientation can be mapped using transverse shear microscopy as had been shown for ultrathin pentacene films.<sup>8</sup> Such measurements have resulted in quantitative grain analyses in some semiconductors.<sup>9,10</sup> The grain growth mechanism in inorganic semiconductors after annealing can be understood with an analytical random nucleation growth process. During this process nucleation sites are randomly chosen, from where the grain can start to grow until it is confined by neighboring grains. Such a process will result in a lognormal-like distribution with important differences in rare events occurring in the tail of the distribution. The differences depend on the film dimensionality (thin film or bulk) and the grain growth rates,<sup>11</sup> and require a large set of grains per sample usually not available from a single image.

Whereas covalent bonds play an important role in the grain formation of inorganics, the relatively weak van der Waals force of organic semiconductors puts less constraints on the morphology. Therefore, the interaction with the substrate type, substrate surface, and the substrate deposition temperature influences the organic crystallite (grain) size and structural thin film characteristics.<sup>12–14</sup> The understanding and control of the film structure would allow to tailor many

other properties that depend on grain boundaries, grain size, and film roughness, such as the carrier mobility and the environmental stability.<sup>15</sup>

Here, a quantitative study of grain size distributions in phthalocyanine thin films is presented, where the substrate deposition temperature is controlled to change the mean crystallite size of the distribution. Previous results have qualitatively shown that the deposition temperature dramatically increases the mean grain size.<sup>3,16,17</sup> We demonstrate that not only the mean size changes, but also the distribution type. The asymmetric molecule gives rise to elongated grains, which can be approximated as ellipses to determine the length of the minor and major axis. Interestingly, at low-deposition temperature, the minor axis is distributed normally, while the major axis follows a lognormal distribution implying that the shape of the molecule modifies the grain size distribution of organic semiconductors. The optimized growth temperature for phthalocyanine thin films is near 200 °C, which achieves large grains with low surface roughness.

**II. EXPERIMENT**

A series of organic thin films were deposited onto c-cut sapphire substrates. The substrates were carefully cleaned with acetone, isopropanol, and methanol in an ultrasonic bath before loading into an organic molecular beam epitaxy system. Additionally, before deposition, the substrates were preheated to 300 °C to remove water and surface impurities. The samples were then deposited at base pressures near  $7 \times 10^{-9}$  Torr. The iron phthalocyanine source material obtained from Sigma-Aldrich had been purified three times with thermal gradient zone sublimation prior to loading into the ultra high-vacuum system. The source material is further outgassed for several hours at 150 °C to improve the film

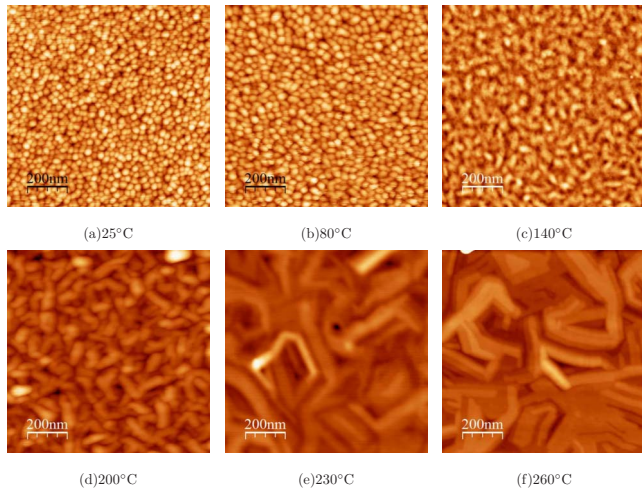


FIG. 1. (Color online) Evolution of AFM images for six iron phthalocyanine thin films with deposition temperatures from 25 to 260 °C. Each AFM image is 1  $\mu\text{m}$  in size. All samples have the same thickness of 27 nm, which is less than the average grain size for all samples. A 20-fold increase in grain area is observed over this temperature range.

quality. For the thin film deposition, the iron phthalocyanine was heated inside a Knudsen cell to 350 °C to obtain an average evaporation rate between 1.0 and 1.6  $\text{\AA}/\text{s}$  for all samples. The rate was measured before and after deposition using a quartz crystal monitor and the rate change was less than 5%. The phthalocyanine thickness was calibrated from Kiessing fringes in the  $\text{Cu } K_{\alpha}$  x-ray diffraction spectrum. The spectrum also shows a prominent (200) FePc peak at the  $2\theta$  angle of  $6.8^{\circ}$ .<sup>18</sup> This angle corresponds to a lattice spacing of 1.3 nm, so that the molecule’s  $b$  axis is oriented parallel to the substrate, but randomly distributed in the plane.

The substrate deposition temperature for the series of samples is varied from room temperature to 260 °C for a fixed thickness of 27 nm, which corresponds to about 20 monolayers of iron phthalocyanine. As the smallest average grain diameter is 35 nm, all films are considered to be two dimensional. Additionally, samples were grown at a fixed substrate temperature of 80 °C with thicknesses ranging from 27 nm up to 216 nm forming multilayer three-dimensional grains.

The morphology of the thin films is investigated with AFM, employing a digital instruments MULTIMODE™ scanning probe microscope in tapping mode. For each sample, several AFM images at high resolution (260 000 pixels) were recorded to accumulate data of at least 3000 grains per sample, see Fig. 1. The grain size was determined by Watershed image segmentation processing.<sup>19,20</sup> The data for a few images were analyzed by eye and compared with a Watershed image processing algorithm. The discrepancy between the two methods was sufficiently small; i.e., the difference in grains found was within 1% and the difference in average size was also within 1%, so that the automated Watershed-based algorithm could be employed to extend the analysis to include data from 84 AFM images for this study. The grain boundaries are outlined and overlaid on the original AFM image in Fig. 2(a). Special care was taken to remove edge

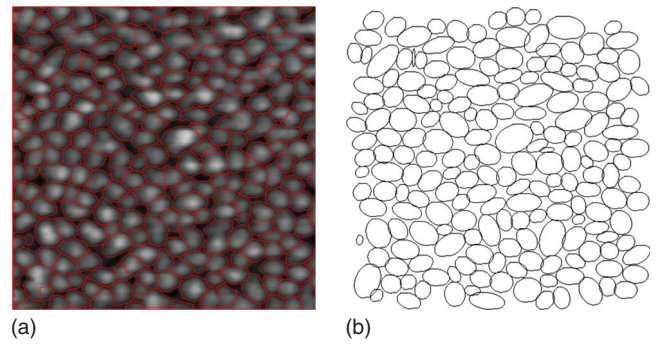


FIG. 2. (Color online) (a) AFM image with overlaid red contours of grain edges as found by the Watershed algorithm. (b) Ellipses of the same size are fit to the grains and edge grains are removed from the image.

grains from the analysis. These grains are only partial grains and would skew any distribution toward lower grain sizes.

Once the contour of each grain is determined, an ellipse with equal area is fitted to the grain, see Fig. 2(b). The minor and major axis of the ellipse are determined as well as the relative orientation of the major axis. No preferential direction of the ellipses’ major axis was observed in any of the samples.

At higher deposition temperature, the grains have a needle-like shape due to the structural anisotropy of the molecule. The molecular plane is perpendicular to the substrate surface, which is evident from separate x-ray diffraction measurements.<sup>16</sup> Separately, a height histogram of this AFM image for the 260 °C sample shows equally spaced peaks. The histogram peaks result from the visible plateaux in Fig. 1(f), where each peak represents an individual molecular level. While the horizontal resolution of the AFM technique is limited by the rounded AFM tip, the vertical resolution can be much better on smooth surfaces without pin holes. The

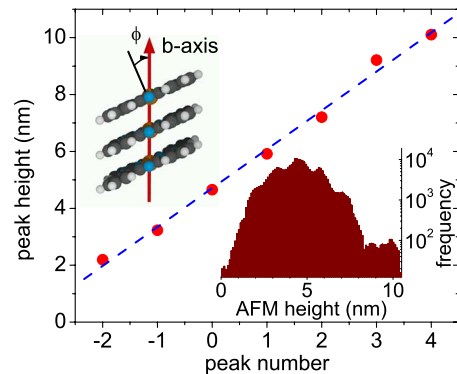


FIG. 3. (Color online) The peak positions of the AFM frequency height plot are graphed for a 27 nm thick iron phthalocyanine film deposited at 260 °C. The frequency distribution (bottom right) shows uniformly spaced peaks that correspond to molecular planes. From a linear fit, the average peak spacing is determined to be 1.36 nm reflecting the size of one monolayer of iron phthalocyanine molecule with the  $b$ -axis parallel to the substrate plane. The inset (top left) shows the stacking angle  $\phi$  that the molecular plane makes with respect to the  $b$ -axis. This is a top view of the molecular arrangement onto the substrate.

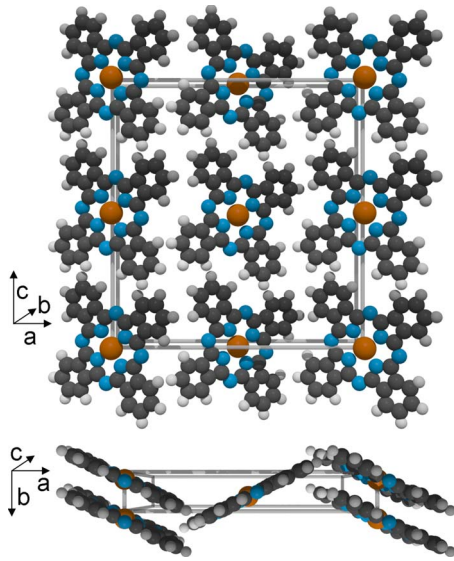


FIG. 4. (Color online) The unit cell of  $\alpha$ -phase iron phthalocyanine contains 4 molecules. The lattice parameters are  $a=25.9$  Å,  $b=3.8$  Å,  $c=24.1$  Å, and  $\beta=90^\circ$ . In the top view the frontal plane of molecules is drawn only for better clarity. The top view shows the  $ac$  plane and the bottom view the  $ab$  plane of the unit cell.<sup>21,22</sup>

average spacing between peaks is  $1.36 \pm 0.05$  nm as determined from a Gaussian multiple-peak fit, see Fig. 3. This spacing is equivalent to an iron phthalocyanine monolayer, where the  $b$  axis is parallel to the substrate plane. This agrees with x-ray diffraction measurements that show a preferential growth direction along the  $b$  axis for all samples. The unit cell of the molecule is drawn in Fig. 4 and shows the typical herringbone structure common in small molecule thin films.

### III. ANALYSIS AND RESULTS

The grain size and shape of organic thin films strongly depends on the growth conditions, in particular on the substrate temperature.<sup>23,24</sup> The adsorbed molecules on the substrate surface can either form nucleation sites or diffuse across the surface to grow islands.<sup>25</sup> Noticeably, this island

growth is asymmetric as the phthalocyanine molecule prefers to stack along the  $b$  axis; i.e., the plane-on-plane configuration has lower energy than the plane-by-plane arrangement.<sup>26</sup> As the deposition temperature is raised from room temperature to 260 °C or close to the resublimation temperature of phthalocyanine, the grains elongate along the major axis ( $b$  axis) and increase in area. The average grain area grows from 2000 to over 45 000 nm<sup>2</sup>, an increase in over 20 times due to the nature of weak van der Waals bonds of organic molecules.<sup>12</sup> Moreover, a size change of 25 times is found considering the largest 10% of grains only, while the major axis increases sixfold and the minor axis increases fourfold for the largest 10% of grains. Each grain is attributed a nominal diameter that represents a circle with the same area. The frequency of grain diameters is summarized in the form of histograms and fitted to distribution functions. Two results of histograms for a low and high-temperature sample exemplify the different distributions in Fig. 5. The sample grown at 25 °C shows an almost symmetric distribution of grains, which can be fitted to a Gaussian (normal) distribution that has a mean grain diameter of 30.8 nm and a standard deviation of 8.2 nm. For a sample of equal thickness deposited at 260 °C, the lognormal distribution is a better fit with a  $\chi^2$  value of 420 as compared to a Gaussian fit, which has a  $\chi^2$  value of 1390. Noticeably important rare events of large grains are more common for samples deposited at high substrate temperatures.

Once the grain distribution is normalized with respect to the mean diameter, then only two distinct grain size distributions emerge (Fig. 6). There is a clear cross over in grain size distribution above 200 °C. This is particularly evident from best  $\chi^2$  fits shown in Table I. While the Gaussian fits are equally good at all temperatures, the lognormal fits become much better at high temperatures. This cross over is accompanied by an abrupt increase of surface roughness. In fact, for samples with deposition temperatures from 25 to 200 °C, the rms surface roughness of a  $1 \times 1$   $\mu\text{m}^2$  image is 1.3 nm on average, see Table I. The roughness for films between 230 and 260 °C is more than double (3.1 nm), also observed earlier.<sup>16</sup> This change in distribution type is indicative of a fundamental change of growth process and a related phase

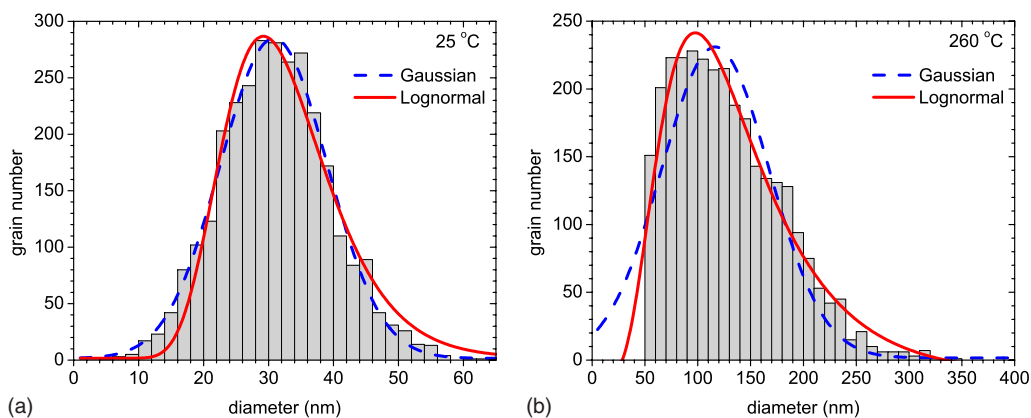


FIG. 5. (Color online) Grain size distributions for two iron phthalocyanine thin films deposited at (a) 25 °C and (b) 260 °C. The diameter corresponds to a nominally circular grain with equal area. For the room temperature sample, the Gaussian fit has a lower  $\chi^2$  value, and for the high-temperature sample, a lognormal distribution follows the experimental data more closely.

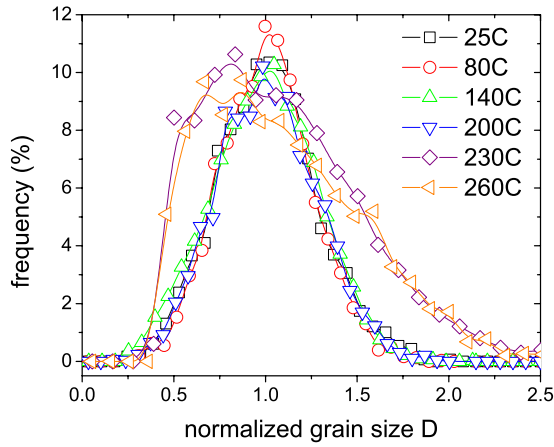


FIG. 6. (Color online) Grain size distributions extracted for over 3000 grains for six samples deposited at different temperatures are normalized with respect to the mean grain diameter. The two distinct distributions stem from the  $\alpha$  to  $\beta$  phase transition that occurs above 200 °C.

transition from the metastable  $\alpha$  phase to the stable  $\beta$  phase.<sup>27</sup> These two phases differ in their distinct stacking angles  $\phi$  illustrated in Fig. 3. These tilt angles are 26.5° and 44.8° for the  $\alpha$  and  $\beta$  phase, respectively.<sup>28,29</sup>

By plotting the temperature dependence (Fig. 7), the grain size area increases almost exponentially. From a linear fit to the Arrhenius plot, one obtains 91 and 74 meV in activation energies for the major axis and minor axis, respectively. The activation energy contains terms from the nucleation and the diffusion energy. Due to the structural phase transition above 200 °C, the activated growth in size may be slowed. Thus, 200 °C is an ideal temperature to achieve large grains with low surface roughness.

Since the phthalocyanine molecule is a planar molecule with a large shape anisotropy, it gives rise to elongated grains. This preferred stacking is consistent with free energy minimization calculations.<sup>26</sup> In fact, the circularity of grains or ratio of minor and major axis decreases monotonously with increasing deposition temperature from 0.71 to 0.47 as shown in Fig. 7. Even though, for low deposition tempera-

TABLE I. Lognormal and normal fit comparison of least fit  $\chi^2$  of nominal grain diameter versus deposition temperature. The normal distribution fits better at low deposition temperature, whereas the lognormal distribution describes the higher temperatures more accurately. The distribution shift is accompanied by a change in the AFM rms roughness for samples deposited above 200 °C.

Deposition temperature (°C)	Normal $\chi^2$	Log-normal $\chi^2$	Roughness (nm)
25	116	384	1.5
80	131	442	1.5
140	52	710	1.2
200	168	365	1.1
230	1352	595	2.6
260	1386	423	3.4

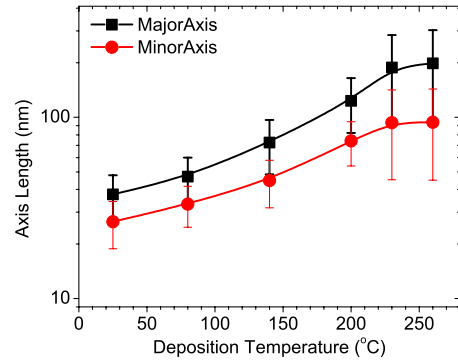


FIG. 7. (Color online) Fitted grain size for minor and major axis versus deposition temperature. The circularity decreases continuously with higher deposition temperatures. The error bars signify the standard deviations of the best fits to the normal or lognormal distributions. Thus, they include 68% of all grains.

ture the grain areas are distributed Gaussian, the major axis distribution cannot be easily fit to the same distribution. In fact rare grains are found, which are above average elongated. In essence, the major axis grain lengths are lognormal distributed while the minor grain axis follows a Gaussian distribution as exemplified in Fig. 8 for a sample grown at 25 °C. For any physical process of multiplying (adding) a series of random variables the outcome tends to be a lognormal (normal) distribution. It is inferred that the anisotropic growth mechanism leads to different grain distributions for minor and major axis.

While major differences in the grain size distributions were found with deposition temperature, the sample thickness varies the grain size only modestly. Samples with different thicknesses deposited at 80 °C showed a slow monotonous increase in roughness and growth in grain diameter from 39 to 52 nm with the FePc film thickness variation from 27 to 216 nm. Again, the major axis of the grain diameter is lognormally distributed, while the minor axis has a normal distribution for all film thicknesses.

IV. CONCLUSION

Quantitative grain size measurements demonstrate the asymmetric grain size growth of a planar organic molecule

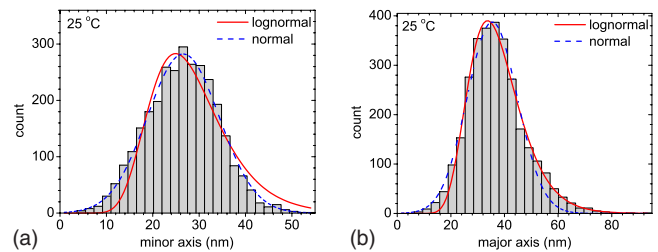


FIG. 8. (Color online) Grain size distributions for a 27 nm iron phthalocyanine sample deposited at room temperature. The grains were fitted to ellipses and their distributions are plotted for the (a) minor and (b) major axis. Using a least  $\chi^2$  fit the normal distribution (dashed) fits better to the minor axis, and the lognormal distribution (line) fits better to the major axis.

with deposition temperature. The average grain area can increase over one order of magnitude in size. In addition the asymmetric growth of iron phthalocyanine hosts unique size distributions along two perpendicular axes in an elliptical model. Since the planar molecule has a preferential growth along its b-axis, it results in a lognormal distribution of the molecules' major axis and a symmetric distribution of the minor axis. The activation energy attributed to the asymmetric growth is 91 and 74 meV for the major and minor axis, respectively. Thus important structural characteristics of or-

ganic semiconductors can be induced by the shape of the molecule in addition to temperature and substrate control.

#### ACKNOWLEDGMENTS

This research was supported by NSF under Grant No. DMR-0847552 and a grant from AFOSR, and the Scholarly and Creative Committee from the College of Natural Science and Mathematics at CSU Long Beach.

\*tgregdig@csulb.edu

- <sup>1</sup>R. D. Yang, T. Gredig, C. N. Colesniuc, J. Park, I. K. Schuller, W. C. Trogler, and A. C. Kummel, *Appl. Phys. Lett.* **90**, 263506 (2007).
- <sup>2</sup>J. Xue, S. Uchida, B. P. Rand, and S. R. Forrest, *Appl. Phys. Lett.* **84**, 3013 (2004).
- <sup>3</sup>M. M. Ling and Z. Bao, *Chem. Mater.* **16**, 4824 (2004).
- <sup>4</sup>G. Horowitz and M. E. Hajlaoui, *Synth. Met.* **122**, 185 (2001).
- <sup>5</sup>S. E. Offerman, N. H. van Dijk, J. Sietsma, S. Grigull, E. M. Lauridsen, L. Margulies, H. F. Poulsen, M. T. Rekveldt, and S. van der Zwaag, *Science* **298**, 1003 (2002).
- <sup>6</sup>B. Stadlober, U. Haas, H. Maresch, and A. Haase, *Phys. Rev. B* **74**, 165302 (2006).
- <sup>7</sup>H. Marom, M. Ritterband, and M. Eizenberg, *Thin Solid Films* **510**, 62 (2006).
- <sup>8</sup>V. Kalihari, E. B. Tadmor, G. Haugstad, and C. D. Frisbie, *Adv. Mater. (Weinheim, Ger.)* **20**, 4033 (2008).
- <sup>9</sup>E. Spiecker, V. Radmilovic, and U. Dahmen, *Acta Mater.* **55**, 3521 (2007).
- <sup>10</sup>Y. Wu, T. Toccoli, N. Koch, E. Iacob, A. Pallaoro, P. Rudolf, and S. Iannotta, *Phys. Rev. Lett.* **98**, 076601 (2007).
- <sup>11</sup>R. B. Bergmann and A. Bill, *J. Cryst. Growth* **310**, 3135 (2008).
- <sup>12</sup>S. R. Forrest and P. E. Burrows, *Supramolecular Science* **4**, 127 (1997).
- <sup>13</sup>S. R. Forrest, *Chem. Rev. (Washington D.C.)* **97**, 1793 (1997).
- <sup>14</sup>C. Kim, K. Bang, I. An, C. Kang, Y. Kim, and D. Jeon, *Curr. Appl. Phys.* **6**, 925 (2006).
- <sup>15</sup>A. B. Chwang and C. D. Frisbie, *J. Appl. Phys.* **90**, 1342 (2001).
- <sup>16</sup>C. W. Miller, A. Sharoni, G. Liu, C. N. Colesniuc, B. Fruhberger, and I. K. Schuller, *Phys. Rev. B* **72**, 104113 (2005).
- <sup>17</sup>T. Nonaka, Y. Nakagawa, Y. Mori, M. Hirai, T. Matsunobe, M. Nakamura, T. Takahagi, A. Ishitani, H. Lin, and K. Koumoto, *Thin Solid Films* **256**, 262 (1995).
- <sup>18</sup>G. Liu, T. Gredig, and I. K. Schuller, *Europhys. Lett.* **83**, 56001 (2008).
- <sup>19</sup>P. Klapetek, I. Ohlídal, D. Franta, A. Montaigne-Ramil, A. Bonanni, and H. S. D. Stifter, *Acta Physica Slovaca* **53**, 223 (2003).
- <sup>20</sup>I. Horcas, R. Fernández, J. M. Gómez-Rodríguez, J. Colchero, J. Gómez-Herrero, and A. M. Baro, *Rev. Sci. Instrum.* **78**, 013705 (2007).
- <sup>21</sup>M. Ashida, N. Uyeda, and E. Suito, *Bull. Chem. Soc. Jpn.* **39**, 2616 (1966).
- <sup>22</sup>J. Buchholz and G. Somorjai, *J. Chem. Phys.* **66**, 573 (1977).
- <sup>23</sup>Y.-L. Lee, W.-C. Tsai, and J.-R. Maa, *Appl. Surf. Sci.* **173**, 352 (2001).
- <sup>24</sup>Z. Bao, A. J. Lovinger, and A. Dodabalapur, *Appl. Phys. Lett.* **69**, 3066 (1996).
- <sup>25</sup>P. Jensen, *Rev. Mod. Phys.* **71**, 1695 (1999).
- <sup>26</sup>S. Yim, S. Heutz, and T. S. Jones, *Phys. Rev. B* **67**, 165308 (2003).
- <sup>27</sup>O. Berger, W.-J. Fischer, B. Adolphi, S. Tierbach, V. Melev, and J. Schreiber, *J. Mater. Sci.: Mater. Electron.* **11**, 331 (2000).
- <sup>28</sup>P. Ballirano, R. Caminiti, C. Ercolani, A. Maras, and M. A. Orru, *J. Am. Chem. Soc.* **120**, 12798 (1998).
- <sup>29</sup>S. Heutz, S. M. Bayliss, R. L. Middleton, G. Rumbles, and T. S. Jones, *J. Phys. Chem. B* **104**, 7124 (2000).